Journal of Catalysis 276 (2010) 85–91

Contents lists available at ScienceDirect

Journal of Catalysis

journal homepage: www.elsevier.com/locate/jcat

Kinetic analysis of cluster size dependent activity and selectivity

Dmitry Yu. Murzin *

Åbo Akademi University, Biskopsgatan 8, Turku/Åbo, Finland

ARTICLE INFO

Article history:
Received 9 July 2010
Revised 2 September 2010
Accepted 3 September 2010

Keywords:
Nanocatalysis
Cluster size effect
Kinetics

ABSTRACT

The impact of nanoparticle size effects in heterogeneous catalytic kinetics over supported metal catalysts is discussed taking into account different activities of edges and terraces. Kinetic equations for the Eley–Rideal mechanism as well as for the two-step sequence were derived, analyzed and compared with experimental data for ethene hydrogenation. Quantitative description for selectivity in a consecutive reaction of pyrrole hydrogenation/ring opening as function of the metal cluster size is provided demonstrating good correspondence between theory and experiments.

1. Introduction

Although the dependence of catalytic activity in transition metal catalysis on changes in the particles size has been a subject of long-term research, recent years witnessed a renaissance in the interest to catalytic properties of materials in the nanometer range, e.g. in the domain between 2 and 20 nm.

The ratio between the surface and volume is enlarged during the reduction in size of nanoparticles, thus the fraction of surface atoms is increasing [1]. Therefore, catalytic activity calculated per total amount of catalytic phase usually declines with the increase of cluster size as fewer exposed sites are available for catalysis. Since changes in the metal particle size lead to alterations of the relative ratio between edges, corners and terrace atoms, as well as changes in the electronic structures, turnover frequency (TOF), defined as the activity per unit of exposed surface, demonstrates not only independence on size (structure insensitivity) but also structure sensitivity [2–10]. Such dependence of TOF in heterogeneous catalytic reactions over metals or metal oxides on the size of clusters (Fig. 1) is currently under intensive investigation.

Less attention in the literature was devoted to analysis of selectivity dependence on the cluster size, although few examples were reported [11,12]. For instance in glycerol oxidation [13] under alkaline conditions, selectivity to the intermediate glycerate increased significantly with the size increase from 3 to 17 nm. Other types of behavior were also reported in the literature. Selectivity in hydrogenation of triple bonds (acetylene [14] or 1-hexyne [15]) over Pd was seen to be independent on the cluster size. It should be, however, noted that according to Anderson et al. [16] under appropriate reaction conditions, samples with higher dispersion of Pd showed intrinsically faster reaction rate in hydrogenation of 1-hexyne, thus the reaction was considered to be size dependent.

Phenylacetylene hydrogenation over gold catalysts [17] exhibited strong dependence of selectivity toward the intermediate product – styrene on cluster size. For example at a similar conversion level, an increase of the size from 2.5 to 30 nm resulted in a substantial decrease of styrene selectivity from 8% to 0.7%.

Similar to hydrogenation of phenylacetylene, in the Fischer–Tropsch reaction selectivity to an intermediate product – methane declined from 30% to 10%, while selectivity for C_{5+} products increased (from 51% to 85%) when the cobalt particle size was increased from 2.6 to 16 nm [18,19].

The effect of the nanoparticle size on the selectivity in cyclohexene hydrogenation/dehydrogenation, and hydrogenation of benzene and crotonaldehyde was discussed [11,12]. In the later case [12], selectivity to crotyl alcohol decreased with the particle size increase. An interesting example of structure sensitivity is carbon–nitrogen ring opening in pyrrole hydrogenation for platinum nanoparticles smaller than 2 nm [20].

It should be, however, emphasized that quantitative analysis of selectivity depending on the particles size is seldom reported, although few attempts can be found in the literature accounting for kinetic features of the cluster size effect based on a thermodynamic approach [21–24].

Speaking in terms of kinetics, let us consider a simple reaction of monomolecular isomerization $A \rightarrow B$ which follows a mechanism

$$\begin{aligned} A + {}^{*} &\leftrightarrow A^{*} \\ A^{*} &\rightarrow B + {}^{*} \end{aligned} \qquad (1)$$

* Fax: +358 2 215 4479.
E-mail address: dmurzin@abo.fi

0021-9517/$ - see front matter © 2010 Elsevier Inc. All rights reserved.
doi:10.1016/j.jcat.2010.09.003

Nomenclature

*	the surface site
$d_{cluster}$	cluster size
$f_{terraces}$, f_{edges}	fractions of terraces and edges
$\Delta G_{ads,terraces}$	Gibss energy of adsorption on terraces
$\Delta G_{ads,edges}$	Gibss energy of adsorption on edges
K_A	adsorption constant of A
k	rate constant k
Z	surface site
α	Polanyi parameter
γ	surface free energy
θ_A	surface coverage, of A
$\mu(r)$	chemical potential
$\mu(\infty)$	chemical potential of a metal particle of an infinite size (bulk-like)
v	the order of a cluster.
χ	parameter in Eq. (17)
ω_I	frequencies of steps
Ω	the atomic volume of the bulk metal.

where * is the surface site, adsorption step is at quasi-equilibrium and the surface reaction is irreversible. The rate is expressed

$$r = k\theta_A = k\frac{K_A C_A}{1 + K_A C_A} \tag{2}$$

where K_A is the adsorption constant and C is concentration of A, respectively.

In the general case of real surfaces with lateral interactions, the rate constant k depends not only on the size of nanocluster r and its morphology, but on surface coverage θ_A, since lateral interactions obviously are more prominent at higher coverage.

In addition to the rate constant, also equilibrium constant can depend on the cluster size, thus coverage can also change with changes of the cluster size.

Mechanistic explanations in the literature, which in principle should account for variations of rate and equilibrium constants with the particles size, include among others [5] variations in the electronic properties of small metal clusters, e.g. more narrow metal valance band, geometric aspects, e.g. changes in the relative fraction of surface sites depending on the cluster size. Another explanation can include presence of metal species with different valencies (i.e. Pt^{4+}, Pt^{2+} and Pt^0) and thus different activity, which relative distribution can alter depending on the cluster size.

In addition, mode of adsorption of mainly complex organic molecules can depend on the cluster size, leading also to changes in the binding energy, which in turn will result in cluster size dependent reaction rates.

Strain or compression was also listed [5] among the possible reasons for the cluster size effect. The latter concept was very much behind the thermodynamic approach [21,22], which albeit being rather formal, was successful in describing experimental data for several heterogeneous catalytic reactions [23,24]. This thermodynamic approach relied on the concept of chemical potential $\mu(r)$, which in a metal particle with a radius of curvature r is different from that in a metal particle of an infinite size (bulk-like) $\mu(\infty)$ in the following way [21,22,25,26]

$$\mu(r) - \mu(\infty) = 2\gamma\Omega/r \tag{3}$$

where γ is the surface free energy and Ω is the atomic volume of the bulk metal. For a liquid, the surface energy excess is then a synonym of the surface tension [27], and the later notion should not be used for solids according to Kolasinki [27]. The treatment of Murzin and Parmon [21–24] assumed that changes of the chemical potential, when the size of nanocluster is changing, are dependent on the presence or absence of an adsorbate.

In the current contribution, we would like to consider a situation when (Fig. 2) the alterations of the chemical potential of nanoclusters in comparison with bulk metal are the same independent on the surface coverage (e.g. bare surface or occupied with reactants). Since differences in the activation energy between edges and terraces are well recognized [7,28], the focus of the paper will be in exploring kinetic consequences of different activities of edges and terraces in terms of reaction rates and selectivity.

2. Geometrical and energetic characteristics of clusters

For the sake of clarity in the following text, we will consider only the terraces and edges, as sites with different reactivity. Thus, for adsorption, an expression for the Gibbs energy can be written

$$\Delta G_{ads} = \Delta G_{ads,terraces} f_{terraces} + \Delta G_{ads,edges} f_{edges} \tag{4}$$

where $\Delta G_{ads,terraces}$ and $\Delta G_{ads,edges}$ correspond, respectively, to adsorption on terraces and edges, while $f_{terraces}$, f_{edges} denote fractions of these surface sites, which sum is obviously equal to unity.

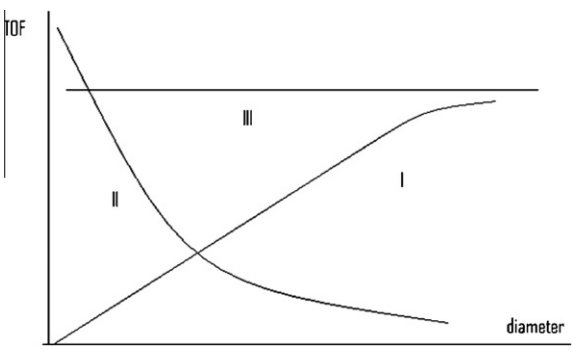

Fig. 1. Structure sensitivity plots. I, II correspond respectively to structure sensitivity, while III represents a structure insensitive reaction.

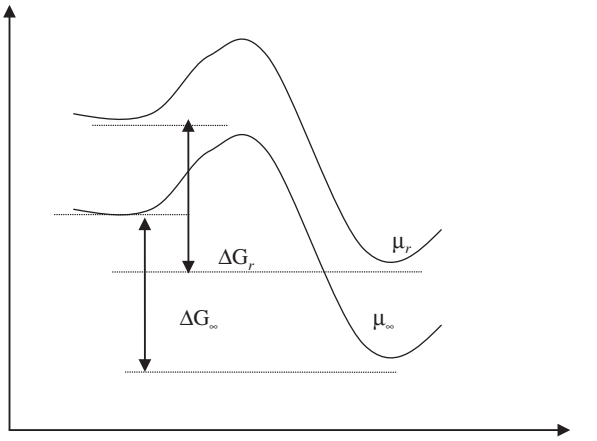

Fig. 2. Energy diagrams illustrating chemical potential differences upon adsorption. The chemical potential $\mu_i(r)$ corresponds to a cluster radius r while μ_∞ denotes a bulk value.

In a more general case, also terraces of different type (e.g. 1 0 0, 1 1 0 or 1 1 1 surfaces) could be considered, as well as other type of surface sites; however, in the current contribution, these sites are lumped and we will initially consider that the reactivity of square and triangular faces in a cubo-octahedron are similar. In the current treatment, the edges between terraces of different type (eq. between (1 0 0) and (1 1 1) and between (1 1 0) and (1 1 1)) are considered non distinguishable. Consideration of edge atoms (along with corner atoms) as active sites was done for instance in [6] for the case of CO oxidation on Au. Although for small molecules the edges could be envisaged as active sites, most probably, for somewhat larger molecules, edge atoms together with terrace atoms constitute an active site. In the present paper, the later extension is not discussed for the sake of clarity.

Eq. (4) can be modified

$$\begin{aligned}\Delta G_{ads} &= \Delta G_{ads,terraces}(1-f_{edges}) + \Delta G_{ads,edges} f_{edges} \\ &= \Delta G_{ads,terraces} + f_{edges}(\Delta G_{ads,edges} - \Delta G_{ads,terraces})\end{aligned} \tag{5}$$

Making use of the relationship between equilibrium constants and Gibbs energy of adsorption one arrives at

$$K_{ads} = e^{\frac{\Delta G_{ads,terraces} + f_{edges}(\Delta G_{ads,edges} - \Delta G_{ads,terraces})}{RT}} \tag{6}$$

Linear free energy (or Brønsted–Evans–Polanyi) relationships are widely used in homogeneously and heterogeneously catalyzed reactions [29–34] in a form which relates reaction constants k with equilibrium constants K in a series of analogous elementary reactions:

$$k = gK^{\alpha} \quad 0 < \alpha < 1 \tag{7}$$

where g and α (Polanyi parameter) are constants. Eq. (7) related transition state properties ($\Delta G^{\neq}$) and those of the initial and final state (ΔG).

Combining Eqs. (6) and (7) an expression for the rate constant of adsorption easily follows

$$\begin{aligned}k_{ads} &= g e^{-\alpha \frac{\Delta G_{ads,terraces} + f_{edges}(\Delta G_{ads,edges} - \Delta G_{ads,terraces})}{RT}} \\ &= g e^{-\alpha \frac{\Delta G_{ads,terraces}}{RT}} e^{\frac{-\alpha f_{edges}(\Delta G_{ads,edges} - \Delta G_{ads,terraces})}{RT}}\end{aligned} \tag{8}$$

which finally takes a form

$$k_{ads} = k'_{ads} e^{\frac{-\alpha f_{edges}(\Delta G_{ads,edges} - \Delta G_{ads,terraces})}{RT}} \tag{9}$$

In order to progress further, geometrical properties of metal clusters should be considered. To this end, a shape, which can represent such a cluster, must be selected. Following [28,35], the cubo-octahedral geometrical model is a good representation of metal clusters often encountered in heterogeneous catalysis. In the studies of supported Pd particles, the cubo-octahedral shape of the particles was fully supported by the high resolution TEM investigation [35]. Certainly, cubo-octahedral geometrical model is a simplification of a true crystal, and it could be argued that this is a statistically improbable occurrence, as most will have a partial outer layer for which many other types of sites or coordination number will appear. Such representation is still probably sufficient for kinetic modeling purposes at least as the first approach. It should be noted that even encapsulated cubo-octahedral Pt nanoparticles can be prepared using for example tetradecyltrimethylammonium bromide as capping agent with a high amount of ideal geometry, as demonstrated in [36], where 90% of particles were cubo-octahedra and just 10% were of irregular shapes.

Expressions for the geometrical characteristics for several structures, including cubo-octahedral one were presented in [37], relating the fractions of edges to the total number of atoms on the surface, which includes besides edges also square and triangular faces

$$f_{edges} = \frac{N_{edges}}{N_{edges} + N_{square\_faces} + N_{triangular\_faces}} \tag{10}$$

Making use of expressions in [37], for cubo-octahedral structures Eq. (10) transforms into

$$f_{edges} = \frac{24(v-1)}{24(v-1) + 6(v-1)^2 + 4(v-1)(v-2)} \tag{11}$$

where v is the order of a cluster. This dimensionless value, which defines the particles size in terms of successive crust added to a pre-existing core, should be related to the cluster size. The fraction of surface atoms in edge sites, excluding those in vertices as a function of the cluster order, is presented in Fig. 3a. It should be noted that the model is not based on a continuously variable particle size.

Number of atoms in one edge, which for cubo-octahedral structure is equal to $v-1$, can be defined as the length of an edge divided by the metal–metal distance. For cubo-octahedral, the cluster diameter is twofold the edge length, thus

$$v - 1 = \frac{d_{cluster}}{2d_{Metal-metal}} \tag{12}$$

Taking as an example distance between Pd–Pd atoms equal to 0.275 nm [35], the fraction of surface atoms in edge sites as function of the cluster size is presented in Fig. 3b. Since the assumed model is not a continuous one, the values of this fraction correspond to cluster sizes with a difference between the neighboring values equal to $2d_{Metal-metal}$ or 0.55 nm in particular case of Pd. For better visibility points, corresponding not to all possible sizes of clusters are given in Fig. 3b. As can be seen from this figure, the fraction of atoms in edges can be described in a simplified way as $f_{edges} \approx 1/d_{cluster}$ when d is given in nm.

It was assumed above that the activity of terraces with different coordination numbers is the same. Generally, it could not be the case, thus it is interesting to analyze the ratio between square and triangular faces as a function of the cluster order. $f_{(square/triangular+square)} = 6(v-1)^2/(4(v-1)(v-2)+6(v-1)^2)$. Such analysis (Fig. 3c) demonstrates that for a cluster order above 3 (ca. 1.1 nm) $f_{square/(square+triangular)}$ is practically independent on the cluster order, thus a direct dependence of the cluster size (nm) into Eq. (9) could be introduced

$$k_{ads} = k'_{ads} e^{\frac{-\alpha(\Delta G_{ads,edges} - \Delta G_{ads,terraces})}{RTd_{cluster}}} \tag{13}$$

where $\Delta G_{ads,terraces}$ defined as $\Delta G_{ads,terraces} = \Delta G_{ads,square\_terraces} f_{square/(square+triangular)} + \Delta G_{ads,triangular\_terraces} f_{triangular/(square+triangular)}$ can be approximately considered as independent on the cluster size.

Interestingly enough, the rate constant of adsorption according to (13) has almost the same dependence on the cluster size as derived in [23,24] using a thermodynamic approach. It can also provide an easy mechanistic explanation for both increase or decrease of adsorption rates with cluster size increase, relating such behavior to Gibbs energy of adsorption on edges and terraces.

3. Two-step reaction sequences

The two-step mechanism with two kinetically significant steps [38,39], which implies that one of the several surface intermediates is the most abundant, while all the others are present on the surface at much inferior concentration levels, is widely applied in the literature to account for heterogeneous catalytic kinetics [40,41]

$$\begin{aligned}&1.\ Z + A_1 \leftrightarrow ZI + B_1 \\ &2.\ ZI + A_2 \leftrightarrow Z + B_2 \\ &A_1 + A_2 \leftrightarrow B_1 + B_2\end{aligned} \tag{14}$$

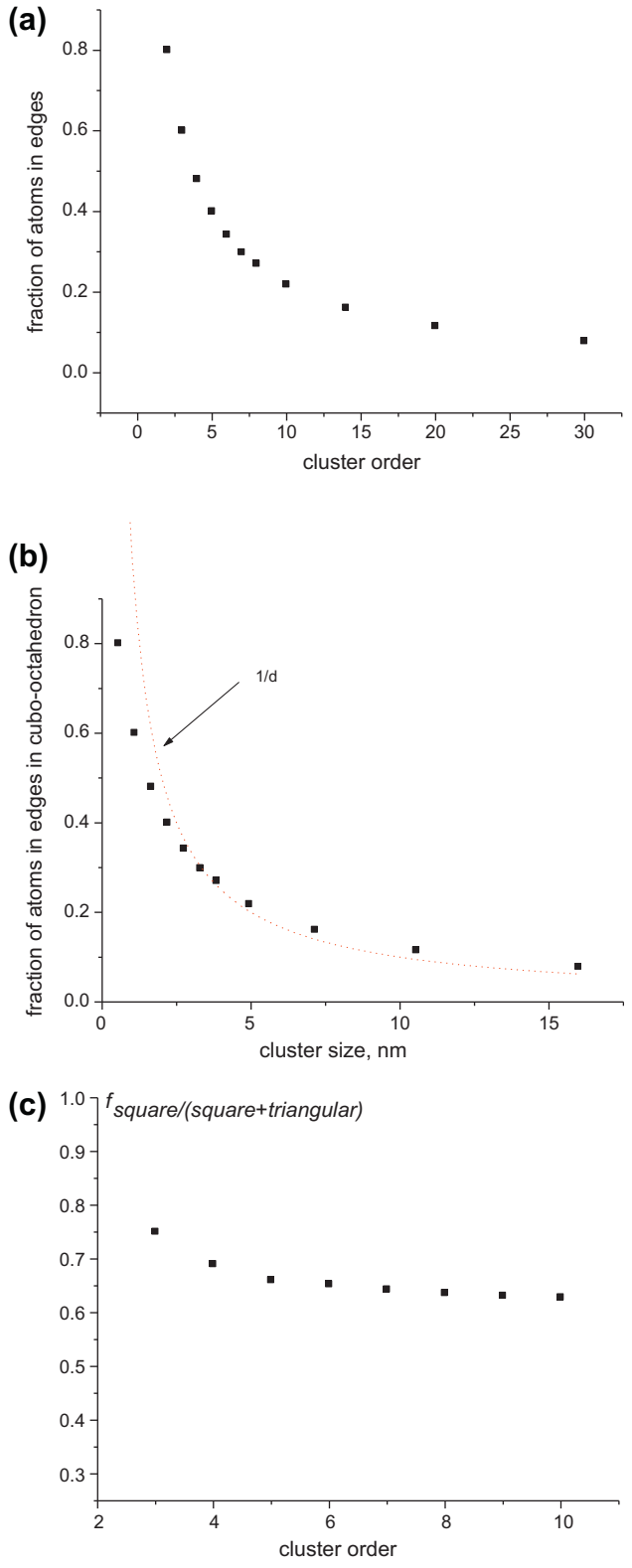

Fig. 3. Fraction of the atoms in edges to the sum of atoms in edges and faces as a function of (a) cluster order and (b) cluster size for cubo-octahedral structure; (c) the ratio of the atoms in square terraces to the total number of atoms in terraces.

where A_1, A_2 are reactants, B_1, and B_2 are products, Z is the surface site and I is an adsorbed intermediate.

The reaction rate for this mechanism is well known [41,42]

$$v(d) = \frac{k_1 P_{A_1} k_2 P_{A_2} - k_{-1} P_{B_1} k_{-2} P_{B_2}}{k_1 P_{A_1} + k_2 P_{A_2} + k_{-1} P_{B_1} + k_{-2} P_{B_2}} \tag{15}$$

where P_{A1}, etc., are partial pressures (for gas-phase reactions) or concentrations (for liquid-phase reactions), k_i – kinetic constants.

The rate constant for the first step of mechanism (14) is

$$k_1(d) = k_1 e^{\frac{-\alpha_1 \chi}{d_{cluster}}} \tag{16}$$

where α_1 is the Polanyi parameter for step 1 and χ is given by

$$\chi = \frac{(\Delta G_{ads,edges} - \Delta G_{ads,terraces})}{RT} \tag{17}$$

Similarly, the rate constant for the backward reaction is

$$k_{-1}(d) = k_{-1} e^{\frac{(1-\alpha_1)\chi}{d_{cluster}}} \tag{18}$$

Analogously, it holds for the second step

$$k_2(d) = k_2 e^{(1-\alpha_2)\chi/d_{cluster}}; k_{-2}(d) = k_{-2} e^{-\alpha_2 \chi/d_{cluster}} \tag{19}$$

Following [40], it can be assumed that $\alpha_1 = \alpha_2 = \alpha$ leading to

$$v(d) = \frac{(k_1 k_2 P_{A_1} P_{A_2} - k_{-1} k_{-2} P_{B_1} P_{B_2}) e^{(1-2\alpha)\chi/d_{cluster}}}{(k_1 P_{A_1} + k_{-2} P_{B_2}) e^{-\alpha\chi/d_{cluster}} + (k_2 P_{A_2} + k_{-1} P_{B_1}) e^{(1-\alpha)\chi/d_{cluster}}} \tag{20}$$

and for an irreversible reaction ($k_{-2} \approx 0$)

$$v(d) = \frac{\omega_2 e^{(1-\alpha)\chi/d_{cluster}}}{1 + \frac{\omega_2 + \omega_{-1}}{\omega_1} e^{\chi/d_{cluster}}} \tag{21}$$

with ω_I are frequencies of steps following the notation of Temkin [41] (the rates of steps (stages) in a particular direction divided by coverage of reacting in this step surface species, i.e. $\omega_1 = k_1 P_{A1}$, etc.). Eley–Rideal mechanism is just a special case of Eq. (21) and can be obtained if the frequency of the second step is assumed to be much slower than ω_{-1}. Eq. (21) can be rewritten as

$$v(d) = \frac{p_1 e^{(1-\alpha)\chi/d_{cluster}}}{1 + p_2 e^{\chi/d_{cluster}}} \tag{22}$$

where $p_2 = (\omega_2 + \omega_{-1})/\omega_1$; $p_1 = \omega_2$.

Eq. (22) in fact was derived in [24] and compared with experimental data. Here, we would like to give just one example related to a case when a maximum in TOF as a function of cluster size was reported [43]. Hydrogenation of ethene on nanoscale catalyst particles at atmospheric conditions was described in [43] with special emphasis on the influence of the Pd particle size on the reactivity at industrially relevant process conditions varying the support and the hydrogen to ethene ratio.

TOF values as a function of Pd particle size for Pd/TiO_2 catalyst at H_2 to C_2H_4 ratios equal to 1:1 and 5:1 were presented for experiments carried out at atmospheric pressure, 293 K and ethene concentration of 8.6×10^{-4} mol l^{-1}. Experimental data [43] are redrawn in Fig. 4 demonstrating a very clear maximum for the stoichiometric ratio between hydrogen and ethene. This figure contains also a comparison between experimental and calculated data according to Eq. (22), confirming good correspondence between experiments and calculations.

No excessive dehydrogenation and coking were mentioned in [43], thus deactivation dependence on the cluster size could be discarded. In general, it could be, however, an important issue, making determinations of TOF challenging.

Certainly, in case of ethene hydrogenation, Eq. (22), which is based on two-step sequence or Eley–Rideal mechanism, might not be the correct one to account for experimental data, thus physico-chemical analysis of the values of kinetic parameters might not be straightforward. As discussed in [23], Langmuir–Hinschelwood type of kinetic expressions could equally well explain a maximum

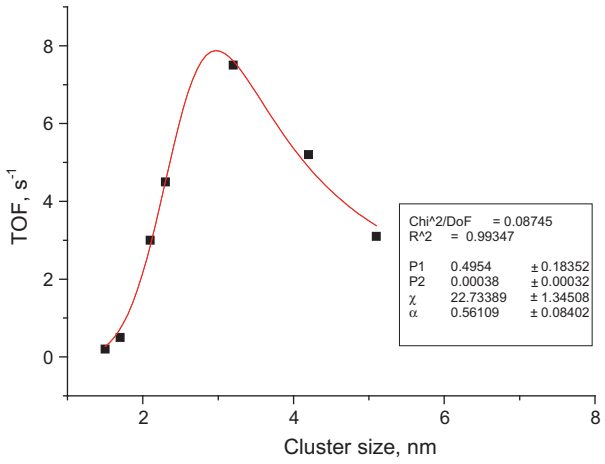

Fig. 4. TOF versus Pd particle radius for Pd/TiO_2 at H_2:C_2H_4 = 1:1 in ethene hydrogenation at 293 K and ethene concentration 8.6×10^{-4} mol l^{-1}. Calculations according to Eq. (22).

in the TOF dependence on the cluster size as a two-step sequence. Thus, in general evaluation of the cluster size effect should be combined with a proper kinetic analysis, when a form of a kinetic equation is established in a reliable way. In any case, the value of Polanyi parameter was close to 0.5 often observed in heterogeneous catalytic reactions, while estimated value of χ leads to a substantial difference between adsorption on edges and terraces, e.g. $\Delta G_{ads,edges} - \Delta G_{ads,terraces}$ is above 55 kJ/mol. Even a larger difference between step-edge sites and terraces of 116 kJ/mol was reported recently in [28].

Theoretical analysis of Eq. (22) clearly shows that the position of the maximum in turnover frequency as a function of cluster size is

$$d_{at\,\max} = \frac{\chi}{\ln \frac{\alpha p_2}{1-\alpha}} \tag{23}$$

depending on the frequencies of steps e.g. on the ratio of $(\omega_2 + \omega_{-1})$ to ω_1, and thus on the partial pressures of the reactants. According to experimental data [43], the maximum activity for Pd/TiO_2 shifts from a Pd particle size of 3 nm for stoichiometric conditions to larger particles sizes of about 4.2 nm for excess of H_2.

It should be noted that although in the analysis of experimental data from [43] only an isothermal case was considered, in general the apparent activation energy can show dependence on the cluster size in agreement with Eq. (22). Such type of experiments were for instance performed for the total oxidation of methane over Pt/Al_2O_3 [44] confirming applicability the thermodynamic approach [21–24], which resulted in an equation similar to Eq. (22). A recent review of Bond [45] addresses various issues of the utilization of kinetics in evaluating mechanisms of heterogeneous catalysis, stressing also that if the apparent activation energy is not constant over the range of a certain variable, the response to that variable will be different at each temperature.

4. Christiansen sequence

An extension of the reaction mechanism discussed above is a Christiansen sequence containing a linear step of isomerization in the adsorbed state [46]

$$\begin{aligned} &1.\ * + A \leftrightarrow *A \\ &2.\ *A \leftrightarrow *B \\ &3.\ *B \leftrightarrow * + B \\ &A \leftrightarrow B \end{aligned} \tag{24}$$

In Eq. (24), step 2 is a linear one. For the purpose of our analysis, steps 1 and 3 are considered as quasi-equilibria. The equilibrium constant of the first step can be determined from Eqs. (16) and (18)

$$K_1(d) = \frac{k_1 e^{\frac{-\alpha_1 \chi}{d_{cluster}}}}{k_{-1} e^{\frac{(1-\alpha_1)\chi}{d_{cluster}}}} = K_1 e^{\frac{-\chi}{d_{cluster}}} \tag{25}$$

Analogously, for the third step

$$K_3(d) = \frac{k_3 e^{\frac{(1-\alpha_3)\chi}{d_{cluster}}}}{k_{-3} e^{\frac{-\alpha_3 \chi}{d_{cluster}}}} = K_3 e^{\frac{\chi}{d_{cluster}}} \tag{26}$$

As the overall constant $K = K_1K_2K_3$ does not depend on the cluster size, it is apparently clear that for the isomerization step 2 in (24) the equilibrium constant as well as the rate constants in forward and reverse directions do not depend on the cluster size, leading finally to the rate expression when the second step is irreversible

$$v = \frac{k_2 K_1 C_A e^{\frac{-\chi}{d_{cluster}}}}{1 + K_1 C_A e^{\frac{-\chi}{d_{cluster}}} + K_3^{-1} C_B e^{\frac{-\chi}{d_{cluster}}}} = \frac{k_2 K_1 C_A e^{\frac{-\chi}{d_{cluster}}}}{1 + (K_1 C_A e + K_3^{-1} C_B)^{\frac{-\chi}{d_{cluster}}}} \tag{27}$$

where coverage of species A is defined as

$$\theta_A = \frac{K_1 C_A e^{\frac{-\chi}{d_{cluster}}}}{1 + (K_1 C_A e + K_3^{-1} C_B)^{\frac{-\chi}{d_{cluster}}}} \tag{28}$$

Analysis of (27) and (28) demonstrates that in principle, the turnover frequency can change with the particle size due to changes in the coverage, while the rate constant will be cluster size independent. Similar type of behavior was recently reported for Fischer–Tropsch synthesis [19].

5. Selectivity dependence on the particle size

For analysis of selectivity in structure sensitive reactions, it is interesting to consider hydrogenation of pyrrole to pyrrolidine and butylamine

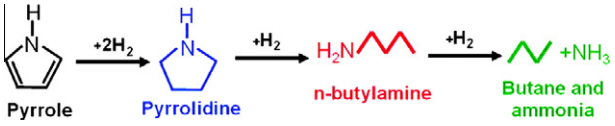

(29)

The first reaction is structure insensitive, while selectivity in butylamine and pyrrolidine depends on the cluster size.

Let us now analyze the consecutive reaction network, which in general is able to explain selectivity in reactions with a similar scheme as in pyrrole hydrogenation

$$\begin{array}{lll} & N(1) & N(2) \\ 1.\ A + Z = ZA & 1 & 0 \\ 2.\ ZA + H_2 \rightarrow B + Z & 1 & 0 \\ 3.\ B + Z = ZB & 0 & 1 \\ 4.\ ZB + H_2 \rightarrow Z + C & 0 & 1 \\ N^{(1)}A \rightarrow B; N^{(2)}B \rightarrow C & & \end{array} \tag{30}$$

where A, B and C stand for pyrrole, pyrrolidine, n-butylamine, respectively. On the right-hand side of the equations for the steps, the stoichiometric numbers along the routes $N^{(1)}$ are $N^{(2)}$ are given. Steps 1 and 3 are considered at quasi-equilibria, thus allowing to write equations for equilibrium constants

$$K_A(d) = K_A e^{\frac{-\chi_A}{d_{cluster}}}, \quad K_B(d) = K_B e^{\frac{-\chi_B}{d_{cluster}}} \tag{31}$$

The rate constants of steps 2 and 4, which are considered irreversible, are respectively

$$k_2(d) = k_2 e^{(1-\alpha_2)\chi_A/d_{cluster}}, \quad k_4(d) = k_4 e^{(1-\alpha_4)\chi_B/d_{cluster}} \tag{32}$$

The reaction rate for consumption of pyrrole is thus given by

$$v_2 = \frac{k_2 e^{(1-\alpha_2)\chi_A/d_{cluster}} K_A e^{\frac{-\chi_A}{d_{cluster}}} C_A C_{H_2}}{1 + K_A e^{\frac{-\chi_A}{d_{cluster}}} C_A + K_B e^{\frac{-\chi_B}{d_{cluster}}} C_B} \tag{33}$$

while the generation rate of butylamine is expressed as

$$v_4 = \frac{k_4 e^{(1-\alpha_4)\chi_B/d_{cluster}} K_B e^{\frac{-\chi_B}{d_{cluster}}} C_B C_{H_2}}{1 + K_A e^{\frac{-\chi_A}{d_{cluster}}} C_A + K_B e^{\frac{-\chi_B}{d_{cluster}}} C_B} \tag{34}$$

The selectivity toward the intermediate product B could be written taking into account (33) and (34)

$$S_B = 1 - \frac{k_4 e^{-\alpha_4 \chi_B/d_{cluster}} K_B C_B}{k_2 e^{-\alpha_2 \chi_A/d_{cluster}} K_A C_A} \tag{35}$$

Assuming that the values of Polanyi parameter are close to each other Eq. (35) can be simplified resulting in

$$S_B = 1 - \frac{k_4 K_B C_B}{k_2 K_A C_A} e^{-\alpha_4(\chi_B - \chi_B)/d_{cluster}} = 1 - p_3 e^{-p_4/d_{cluster}} \tag{36}$$

where p_3 stands for $k_4 K_B C_B / k_2 K_A C_A$, while p_4 is equal to $\alpha_4(\chi_B - \chi_A)$.

Eq. (36) provides a possibility to evaluate dependence of selectivity on the particle size. When the difference in adsorption behavior of pyrrole on terraces and edges is not the same as this difference for pyrrolidine, it can be expected that selectivity will depend on the cluster size. Let us consider now the experimental data reported in [20]. Selectivity to the intermediate pyrrolidine decreased significantly with the size increase from 1 to 3 nm.

Comparison between experimental and calculated values of selectivity toward pyrrolidine done with Origin 7.5 software is presented in Fig. 5. As can be seen from Fig. 5, the trends in selectivity are described in a rather accurate way. As pyrrole to pyrrolidine hydrogenation is structure insensitive, within the framework of the model, developed here, it means that $\chi_A \approx 0$. Assuming the value of Polanyi parameter equal to 0.5, the value of $\Delta G_{ads,edges} - \Delta G_{ads,terraces}$ for pyrrolidine adsorption is close to 2.5 kJ/mol.

Finally note that parameters χ_B and χ_A depend on temperature, indicating also that temperature dependence of selectivity might be different depending on the cluster size.

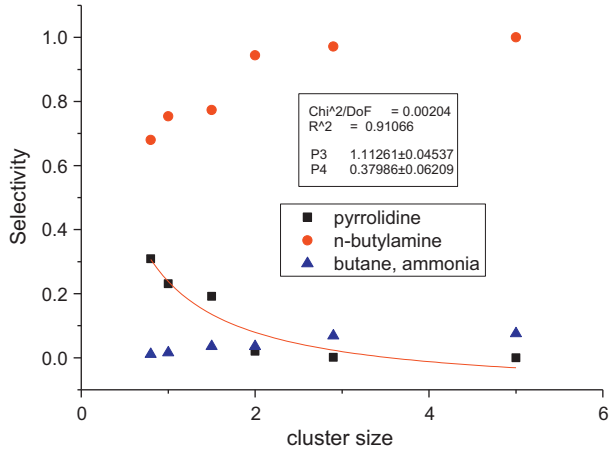

Fig. 5. Measured [20] and modeled (Eq. (36)) selectivity toward pyrrolidine in hydrogenation of pyrrole over well-defined platinum nanoparticles prepared using dendrimer and polymer capping agents and supported onto mesoporous SBA-15 silica.

6. Conclusions

The ability to control particle size of metal catalysts in the nanometer range allows examining the issue of structure sensitivity with well-defined nanoparticles. Difference in reactivity of edges and terraces is supposed in the present work to be responsible for cluster size effects. The ratio between edges and terraces was calculated for cubo-octahedral clusters and shown to be approximately proportional to the reciprocal value of the cluster diameter. Kinetic equations were derived for two-step sequence assuming one most abundant surface intermediate and for several variations of this mechanism. The theoretical concept advanced in the present contribution leads to the same kinetic equations, previously derived [23,24] using a formal thermodynamic approach based on the changes of chemical potential. Comparison between experimental and calculated data performed in [23,24] demonstrated applicability of the kinetic equations to treat experimental data showing increase, decrease and even maxima in TOF as a function of cluster size. An example of such comparison for hydrogenation of ethene on nanoscale catalyst particles at atmospheric conditions was presented in this paper, showing that a substantial difference between adsorption on edges and terraces could be anticipated based on this kinetic analysis. Analysis of a mechanism with a linear step of isomerization in the adsorbed state (Christiansen sequence) demonstrated that turnover frequency can change with the particle size due to changes in the coverage, while the rate constant is cluster size independent in line with recent experimental observations for Fischer–Tropsch synthesis on cobalt.

Finally, a quantitative analysis of selectivity was done for structure sensitive ring opening of pyrrole to *n*-butylamine through formation of pyrrolidine.

Acknowledgments

The author is grateful to Profs. G. Somorjai, E. Iglesia, V. Parmon, V. Bukhtiyarov, A. Stakheev for valuable discussions on various topics related to cluster size effect.

References

[1] R. van Hardeveld, F. Hartog, Surf. Sci. 15 (1969) 189.
[2] A.T. Bell, Science 299 (2003) 1688.
[3] R. Schlögl, S.B. Abd Hamid, Angew. Chem. Int. Ed. 43 (2004) 1628.
[4] R. Narayanan, M.A. El-Sayed, Top. Catal. 47 (2008) 15.
[5] F. Klasovsky, P. Claus, in: B. Corain, G. Schmid, N. Toshima (Eds.), Metal Nanoclusters in Catalysis and Materials Science: The Issue of Size Control, Elsevier, Amsterdam, 2008, pp. 167–181.
[6] B. Hvolbæk, T.V.W. Janssens, B.S. Clausen, H. Falsig, C.H. Christensen, J.K. Nørskov, Nanotoday 2 (2007) 17.
[7] R.A. van Santen, Acc. Chem. Res. 42 (2009) 57.
[8] M. Che, C.O. Bennett, Adv. Catal. 36 (1989) 55.
[9] C.R. Henry, Appl. Surf. Sci. 164 (2000) 252.
[10] M. Boudart, Adv. Catal. 20 (1969) 153.
[11] G.A. Somorjai, J.Y. Park, Angew. Chem. Int. Ed. 47 (2008) 9161.
[12] G.A. Somorjai, J.Y. Park, Top. Catal. 49 (2008) 126.
[13] N. Dimitratos, J.A. Lopez-Sanchez, D. Lennon, F. Porta, L. Prati, A. Villa, Catal. Lett. 108 (2006) 147.
[14] M. Ruta, N. Semagina, L. Kiwi-Minsker, J. Phys. Chem. C 112 (2008) 13635.
[15] N. Semagina, A. Renken, L. Kiwi-Minsker, J. Phys. Chem. C 111 (2007) 13933.
[16] J.A. Anderson, J. Mellor, R.P.K. Wells, J. Catal. 261 (2009) 208.
[17] S.A. Nikolaev, V.V. Smirnov, Gold Bull. 42 (2009) 182;
S.A. Nikolaev, V.V. Smirnov, Catal. Today 147S (2009) S336.
[18] G.L. Bezemer, J.H. Bitter, H.P.C.E. Kuipers, H. Oosterbeek, J.E. Holewijn, X. Xu, F. Kapteijn, A.J. Van Dillen, K.P. de Jong, JACS 128 (2006) 3956.
[19] J.P. den Breejen, P.B. Radstake, G.L. Bezemer, J.H. Bitter, V. Frøseth, A. Holmen, K.P. de Jong, JACS 131 (2009) 7197.
[20] J.N. Kuhn, W. Huang, C.-K. Tsung, Y. Zhang, G.A. Somorjai, JACS 130 (2008) 14026.
[21] V.N. Parmon, Doklady, Phys. Chem. 413 (2007) 42.
[22] V.N. Parmon, Thermodynamics of Non-Equilibrium Processes with a Particular Application to Catalysis, Amsterdam, Elsevier, 2010.
[23] D.Yu. Murzin, Chem. Eng. Sci. 64 (2009) 64.
[24] D.Yu. Murzin, J. Mol. Catal. A. Chem. 315 (2010) 226.
[25] S. Parker, C.T. Campbell, Phys. Rev. B 75 (2007) 035430.

[26] C.T. Campbell, S.C. Parker, D.E. Starr, Science 298 (2002) 811.
[27] K.W. Kolasinki, Surface Science. Fundamentals of Catalysis and Nanoscience, Wiley, Chichester, 2002.
[28] R. van Santen, in: A. Cybulski, J.A. Moulijn, A. Stankiewicz (Eds.), Novel Concepts in Catalysis and Chemical Reactors: Improving the Efficiency for the Future, Wiley, Weinhem, 2010, pp. 1–30.
[29] N. Brønsted, Chem. Rev. 5 (1928) 231.
[30] L.P. Hammett, Physical Organic Chemistry, McGraw-Hill Book Co Inc., New York, NY, 1940.
[31] M.G. Evans, M. Polanyi, Trans. Faraday Soc. 34 (1938) 11.
[32] A. Logadottir, T.H. Rod, J.K. Nørskov, B. Hammer, S. Dahl, C.J.H. Jacobsen, J. Catal. 197 (2001) 229.
[33] D. Loffreda, F. Delbecq, F. Vigné, P. Sautet, Angew. Chem. Int. Ed. 48 (2009) 8978.
[34] R.A. van Santen, M. Neurock, S.G. Shetty, Chem. Rev. 110 (2010) 2005.
[35] G. Agostini, R. Pellegrini, G. Leofanti, L. Bertinetti, S. Bertarione, E. Groppo, A. Zecchina, C. Lamberti, J. Phys. Chem. C 113 (2009) 10485.
[36] K.M. Bratlie, H. Lee, K. Komvopoulos, P. Yang, G.A. Somorjai, Nanoletters 7 (2007) 3097.
[37] J.M. Montejano-Carrizales, F. Aguilera-Granja, J.L. Moran-Lopez, Nanostruct. Mater. 8 (1997) 269.
[38] M.I. Temkin, Kinet. Katal. 25 (1984) 299.
[39] M. Boudart, K. Tamaru, Catal. Lett. 9 (1991) 15.
[40] M. Boudart, Kinetics of Chemical Processes, Prentice-Hall, Englewood Cliffs, NJ, 1968.
[41] M.I. Temkin, Adv. Catal. 28 (1979) 173.
[42] D.Yu. Murzin, T. Salmi, Catalytic Kinetics, Elsevier, 2005.
[43] A. Binder, M. Seipenbusch, M. Muhler, G.J. Kasper, J. Catal. 268 (2009) 150.
[44] I.E. Beck, V.I. Bukhtiyarov, I.Yu. Pakharukov, V.I. Zaikovsky, V.V. Kriventsov, V.N. Parmon, J. Catal. 268 (2009) 60.
[45] G.C. Bond, Catal. Rev. Sci. Eng. 50 (2008) 532.
[46] F.G. Helfferich, Kinetics of homogeneous multistep reactions, in: R.G. Compton, G. Hancock (Eds.), Comprehensive Chemical Kinetics, vol. 38, Elsevier, Amsterdam, 2001.